Available online at www.elixirpublishers.com (Elixir International Journal)

Computational Chemistry

Elixir Comp. Chem. 129 (2019) 52983-52988

ISSN: 2229-712X

Experimental and Theoretical Approach of L - Methionine Sulfone (LMS) as corrosion inhibitor for mild steel in HCL Solution

Ekerete Jackson[1] and K. E. Essien[2]

[1] Department of Chemistry, Faculty of Science, University of Uyo, P.M.B 1017, Uyo, Akwa Ibom State, Nigeria.

[2] Department of Science Technology, Akwa Ibom State Polytechnic, Ikot Osurua, P. M. B. 1200, Akwa Ibom State, Nigeria.

ARTICLE INFO

Article history:

Received: 08 December 2018;

Received in revised form:

22 March 2019;

Accepted: 2 April 2019;

Keywords

L - METHIONINE SULFONE (LMS),

Electrochemical Impedance Spectroscopy,

Corrosion Inhibition.

ABSTRACT

The corrosion inhibition and adsorption processes of L - METHIONINE SULFONE (LMS) on mild steel in 2 HCl was studied by means of chemical (weight loss), electrochemical and quantum chemical techniques. The inhibition efficiency increases with decreasing temperature and increasing concentration of inhibitor. It has been determined that the adsorption of LMS on mild steel obeys the Temkin adsorption isotherm at all studied temperatures with negative values of ΔG^{o}_{ads}, suggesting a stable and a spontaneous inhibition process. In potentiodynamic polarization, the curves shifted towards lower current density in the presence of LMS with well-defined Tafel regions suggesting that the inhibitor retard the corrosion process without changing the mechanism of the corrosion process; and exhibit cathodic and anodic polarization (mixed type inhibitors) because the change in E_{corr} is less than 85 vM/SCE with respect to the blank. Corrosion current density was calculated by extrapolation of the linear parts of these curves to the corresponding corrosion potential; and corrosion potential (E_{corr}), corrosion current densities (i_{corr}), anodic Tafel slope (βa), cathodic Tafel slope (βb) were determined with maximum value of inhibition efficiency for 5 x 10^{-4} M concentration of the inhibitor at 303 K is 75.1%. From Nyquist plots of electrochemical impedance spectroscopy, value of polarization resistance (R_p) increased with increasing inhibitor concentration whereas double layer capacitance (C_{dl}) decreased indicating a decrease in local dielectric constant or an increase in thickness of electric double layer suggesting that the inhibitors function by forming a protective layer at the metal surface. Inhibition efficiency value (η %) is 55.9%. Quantum chemical calculations were performed using Density Functional Theory (DFT) with the help of complete geometry optimization for theoretical calculations of E_{HOMO}, E_{LUMO}, and energy gap (ΔE). Inhibition efficiency increases with increasing E_{HOMO} indicating that the molecule has tendency to donate electrons to the appropriate acceptor molecule with low energy empty molecular orbital; whereas low value of E_{LUMO} suggests that the molecule easily accepts electrons from donor molecules.

1. Introduction

Corrosion is a major concern globally due to the destructive attack of metals by chemical and electrochemical reactions. Though corrosion action seems slow and negligible, it is complex to analyze because it involves a large number of variables. Corrosion is defined as the process in which a metal or its alloy is consistently transformed from the pure metallic form to the oxidized state by interacting with the environment [1,2].

Corrosion can take place in different media: acidic, alkaline or neutral; and in various ways either over the entire surface of the metal, electrochemically between the different metals or between two points on the metal surface that have different chemical activity. Corrosion consists of at least two reactions on the surface of the corroding metal; one is the oxidation, also referred to as anodic half reaction; the other is reduction reaction, also referred to as cathodic half reaction [2]

Negligence of the basic corrosion protection technology can lead to expensive problems not only financial but also with respect to safety as well. This is why anti-corrosion techniques are of much importance and they can be determined at two levels: prevention at the stage of design, the “cure” stage after corrosion has set in. These include engineering design, anodic protection, lining, cathodic protection and corrosion inhibition. Corrosion control of metals is of technical, economic, environmental, and aesthetical importance. The use of inhibitors is one of the best options of protecting metals and alloys against corrosion [3].

Organic compounds have long been known to inhibit the corrosion of mild steel in acidic media. Organic compounds previously studied as inhibitors include triazole derivatives [4], bipyrazolic derivatives [5], aromatic hydrazides [6], organic dyes [7,8], poly(4-vinylpyridine) [9] and thiosemicarbazide [10].

Tele:

E-mail address: ekeretejackson@yahoo.com

These compounds can adsorb onto the mild steel surface and block active sites, thus decreasing the corrosion rate. Most well-known acid inhibitors are organic compounds containing nitrogen, sulfur, and oxygen atoms. Among them, nitrogen-containing heterocyclic compounds are considered to be effective corrosion inhibitors on steel in acid media [11]. N-heterocyclic compound inhibitors act by adsorption on the metal surface, and the adsorption as well as those with triple or conjugated double bonds or aromatic rings in their molecular structures.

Thus, the inhibitory effect of **L - METHIONINE SULFONE** on mild steel corrosion in 2 M HCl at 303 -333 K was studied by weight loss as well as by quantum chemical studies. The inhibitor adsorption mechanism was studied, and the thermodynamic functions for the dissolution and adsorption processes were calculated and discussed. The choice of this compound was also based on molecular structure considerations and has not been investigated as corrosion inhibitor.

The molecular structure of **L - METHIONINE SULFONE (LMS)** is as shown below:

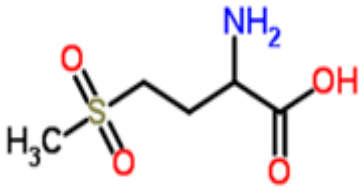

Figure 1. The chemical structure of L - METHIONINE SULFONE (LMS).

2. Experimental Method

2.1 Mild steel

The coupons were mechanically pressed cut into 2 by 1.5 cm measurement and a hole was made for insertion of the hooks. The coupons were polished with series of emery paper of variable grades starting with the coarsest and then proceeding in steps to the finest (600) grade, degreased with ethanol, dipped in acetone and stored in a desiccator [12, 13, 14, 15].

Table 1. Chemical Composition of Mild Steel Samples (Wt %).

C	0.17
Si	0.26
Mn	0.46
P	0.0047
S	0.017
Fe	Bal.

2.2. Solution

Solution of 2 M HCl was prepared by dilution of 98% HCl (Analytical grade) using distilled water. LMS was added to the acid in concentrations ranging from 0.5 µM to 5.0 µM and the solution in the absence of LMS was taken as blank for comparison. Tests were conducted under total immersion conditions in 100 ml of test solutions maintained at 303 – 333 K. The pre-cleaned and weighed coupons were immersed in beakers containing the test solutions. To determine weight loss with respect to time, the coupons were retrieved from test solutions at 2 hrs intervals progressively for 10hrs, immersed in 20% NaOH solution containing $200gl^{-1}$ of zinc dust, washed in distilled water, dried in acetone and re-weighed. The weight loss was taken to be the difference between the weight of the coupons at a given time and its initial weight of the test coupon determined using LP 120 digital balance with sensitivity of ±1 mg.

2.3. Gravimetric measurements

The apparatus and procedure followed for the weight loss measurements were as previously reported [16-20]. The corrodent concentration was kept at 2 M HCl and the volume of the test solution used was 100 mL. All tests were made in aerated solutions. The difference between the weight at a given time and the initial weight of the coupons was taken as the weight loss which was used to compute the corrosion rate given by [17]:

$$\text{Corrosion rate, } \rho = \frac{\Delta W}{At} \quad (1)$$

Where, ΔW is the weight loss, A is the total area of the mild steel coupon, t is the corrosion time and ρ is the corrosion rate.

$$\text{Surface Coverage, } \theta = \frac{\rho_1 - \rho_2}{\rho_1} \quad (2)$$

$$\text{Inhibition efficiency, \% I} = \frac{\rho_1 - \rho_2}{\rho_1} \times 100 \quad (3)$$

Where ρ_1 and ρ_2 are the corrosion rates of the mild steel in 2 M HCl (blank) in the absence and presence of inhibitor respectively.

2.4 Polarization measurement

The working electrode was immersed in test solution during 30 minutes until a steady state open circuit potential (E_{ocp}) was obtained. The polarization curve was recorded under potentiodynamic polarization conditions and under air atmosphere and it was controlled by a personal computer. After the open circuit potential had been established, dynamic polarization curves were obtained at a scan rate of 1 mV/s in the potential range from - 0.25 V to 0.25 V. Corrosion current density (i_{corr}) values were obtained by the Tafel extrapolation method. All potentials were measured against SCE. The percentage inhibition efficiency (η), was calculated using the equation [21]

$$\eta(\%) = \frac{i^o_{corr} - i_{corr}}{i^o_{corr}} \times 100 \quad 4$$

where i^o_{corr} and i_{corr} are values of corrosion current density in the absence and presence of inhibitor respectively.

2.5 Electrochemical impedance spectroscopy measurement

The electrochemical impedance spectroscopy measurements were carried out over a frequency domain from 10 Hz to 100,000 Hz at 303 K using amplitude of 5 mV RMS peak to peak with an ac signal at the open circuit potential and an air atmosphere. The impedance data were obtained using Nyquist plots and the polarization resistance R_p was obtained from the diameter of the semicircle in Nyquist plot. The polarization resistance (R_p) includes charge transfer resistance (R_{ct}), diffuse layer resistance (R_d), the resistance of accumulated species at the metal/solution interface (R_a) and the resistance of the film (in the presence of the inhibitor) at the metal surface (R_f). The percentage inhibition efficiency (η) was calculated from the polarization resistance values obtained from the impedance measurements according to the relation [22]

$$\eta(\%) = \frac{R_p(inh) - R_p}{R_p(inh)} \quad x \quad 100 \qquad 5$$

where $R_{p(inh)}$ and R_p are the charge transfer resistance in the presence and absence of inhibitor respectively. The double layer capacitance (C_{dl}) was calculated using the equation

$$C_{dl} = \frac{1}{2\pi f_{max} R_p} \qquad 6$$

where f_{max} is the frequency at the maximum in the Nyquist plot.

2.6 Theoretical and computational chemistry

First principle calculations were carried out using density functional theory (DFT) under the generalized gradient approximation (GGA) with Perdew – Burke - Eruzerhof (PBF) exchange correlation functional as implemented in Dmol^3 module using material studio software package version 6.0. The quantum chemical indices considered were: the energy of the highest occupied molecular orbital (E_{HOMO}), the energy of the lowest unoccupied molecular orbital (E_{LUMO}), Energy gap = E_{HOMO} - E_{LUMO}, total energy, and Mulliken charges [23].

3. Results and Discussion

3.1. Weight loss, corrosion rate and inhibition efficiency

The weight loss (gravimetric measurements) for the mild steel in 2 M HCl containing different concentrations of LMS as function of time at 303 K is presented in Fig. 2.

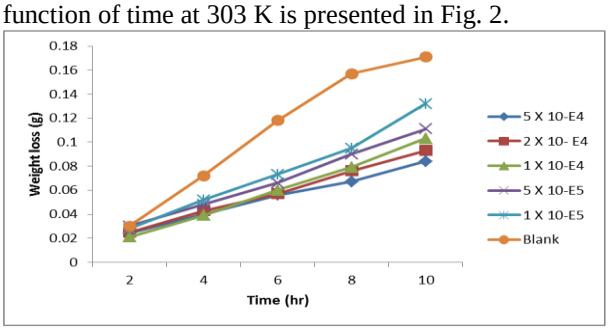

Fig. 2.Variation of weight loss with time for the corrosion of mild steel in 2 M HCl containing various. concentrations of concentrations of LMS at 303 K.

3.2 Weight loss measurement

The corrosion inhibition efficiency (% IE), corrosion rate (CR) and surface coverage (Θ) of **L - METHIONINE SULFONE (LMS)** after 10 hours of immersion at different temperatures (303 to 333K) are presented in Table 1. It is observed that the inhibition efficiency increased with increasing concentration of the inhibitor. In the absence of any inhibitor, the corrosion rate of mild steel increased steeply with increase in temperature. The corrosion rate was much lower in the presence of inhibitors than in the absence of any inhibitor at any temperature resulting in the retardation of the rate at which the metal goes into solution. The plot of weight loss versus time between 303 K and 333 K for the blank and various concentrations of the inhibitor are shown in FIG. 2. For the blank (2 M HCl) the graph is uppermost due to the high corrosion rate; and the lower graphs are for various concentrations of the inhibitor indicating inhibition (reduction in corrosion rate) with increasing inhibitor concentrations.

3.3 Adsorption / Thermodynamic studies

The adsorption characteristics of the inhibitor (LMS) were investigated by fitting data obtained for the degree of surface coverage in different adsorption isotherms. The test indicated that the adsorption was best described by Temkin adsorption model which is expressed as

$$\exp(f\theta) = K_{ads}C \qquad (7)$$

K_{ads} is the equilibrium constant of the adsorption process, C is the inhibitor concentration, Θ is the surface coverage, and f is the factor of energetic inhomogeneity.

FIG. 5 is a plot of surface coverage against logarithm of inhibitor concentration. The correlation coefficient (R^2) was in the range 0.963 to 0.997 for all the inhibitors which is close to unity, indicating that the adsorption of the inhibitors is consistent with Temkin adsorption model.

The parameter f is defined as

$$f = -2a \qquad (8)$$

where a is molecular interaction parameter. The calculated values of a and equilibrium constant of the adsorption process (K_{ads}) obtained from Temkin adsorption plots are shown in table 3.

$$\exp(-2a\theta) = K_{ads}C \qquad (9)$$

The sign between f and a is reverse; that is, if $a < 0$, $f > 0$ and if $a > 0$, $f < 0$, mutual repulsion of molecules occurs,but if $f < 0$ attraction occurs [24].

K_{ads} denotes the strength between adsorbate and adsorbent. Large values of K_{ads} indicate more efficient adsorption and better inhibition efficiency. From table 4, values of K_{ads} are very low which indicate weak interaction between inhibitor and mild steel surface.

$$K_{ads} = \frac{1}{55.5}\exp\left(\frac{\Delta G^{\circ}_{ads}}{RT}\right) \qquad (10)$$

Where R is the molar gas constant, T is temperature and 55.5 is concentration of water in solution expressed in molar.

$$\log K_{ads} = 1.744 - \frac{\Delta G^{\circ}_{ads}}{2.303RT} \qquad (11)$$

The standard free energy of adsorption (ΔG^{o}_{ads}) was calculated from the above equation and presented in table 4. The positive values of the ΔG^{o}_{ads} reflect the non spontaneity of the adsorption process and stability of the adsorped layer on the mild steel.

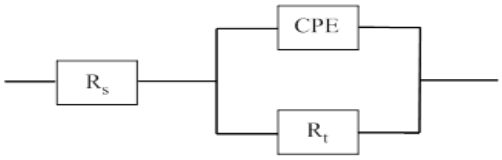

Fig. 3. Temkin isotherm for the adsorption of LMS on mild steel surface.

Table 2. Temkin parameters for the adsorption of LMS on mild steel surface at 303 - 333 K.

Inhibitor	T (K)	Intercept	Slope	K x 10^{-4} (mol/L)	f	a	ΔG (kJ/mol)	R^2
LMS	303	0.591	- 0.067	1.43	- 14.725	7.463	32.34	0.963
	313	0.622	- 0.066	0.44	- 15.152	7.576	34.98	0.965
	323	0.699	- 0.065	0.40	- 15.385	7.693	38.42	0.966
	333	0.814	- 0.076	0.24	- 13.158	6.579	40.67	0.997

TABLE 3. Calculated values of corrosion rate of mild steel (CR), degree of surface coverage (Θ) and inhibition efficiency (% IE) of LMS at 303 to 333K.

Inhibitor	Conc. x 10^{-4} (M)	303 K			313 K			323 K			333 K		
		CR $gcm^{-2}m^{-I}$ x 10^{-4}	Θ	% IE	CR $gcm^{-2}m^{-I}$ x10^{-4}	Θ	% IE	CR $gcm^{-2}m^{-I}$ x 10^{-4}	Θ	% IE	CR $gcm^{-2}m^{-I}$ x 10^{-4}	Θ	% IE
	BLANK	8.55	-	-	12.75	-	-	19.60	-	-	29.60	-	-
LMS	5.0	4.20	0.51	51	5.73	0.55	55	7.65	0.61	61	7.70	0.74	74
	2.0	4.65	0.46	46	6.50	0.49	49	9.25	0.53	53	10.10	0.66	66
	1.0	5.15	0.40	40	7.39	0.42	42	10.60	0.46	46	12.75	0.58	58
	0.5	5.55	0.35	35	7.77	0.39	39	10.97	0.44	44	14.25	0.52	52
	0.1	6.58	0.23	23	9.35	0.27	27	13.15	0.33	33	16.90	0.43	43

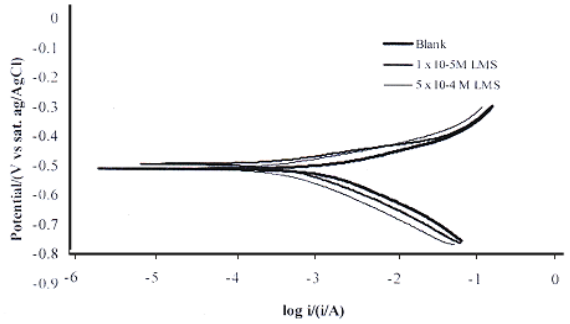

Fig. 4. Potentiodynamic polarization curve for mild steel in 2 M HCl in the presence and absence of L - METHIONINE SULFONE (LMS) at 30^0C.

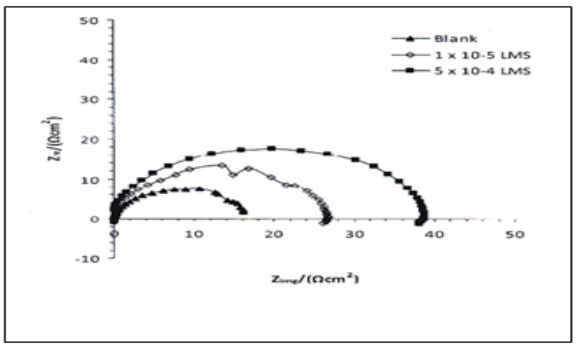

Fig. 5.Nyquist plot for the corrosion of mild steel in 2 M HCl solution in the absence and presence of L - METHIONINE SULFONE (LMS) at 30^0C.

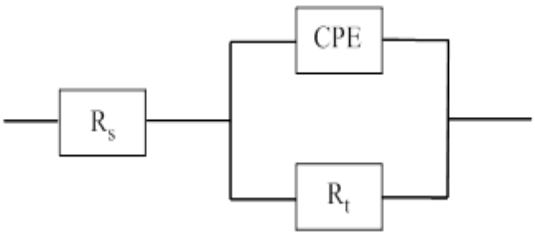

Fig.6. Equivalent circuit for MS in 2M HCL Solution.

3.4 Electrochemical Impedance Study (EIS)

The electrochemical impedance data are depicted as Nyquist plot in Fig. 3. Analysis of the Nyquist plot (fig. 3) showed a depressed capacitance loop which arises from the time constant of the electrical double layer and charge transfer resistance. The deviation of semicircles from perfect circular shape is often referred to the frequency dispersion of interfacial impedance [25]. This behavior is usually attributed to the inhomogeneity of the metal surface arising from surface roughness or interfacial phenomena [26], which is typical for solid metal electrodes [27]. The polarization resistance R_p was obtained from the diameter of the semicircle in Nyquist plot. The polarization resistance (R_p) includes charge transfer resistance (R_{ct}), diffuse layer resistance (R_d), the resistance of accumulated species at the metal/solution interface (R_a) and the resistance of the film (in the presence of the inhibitor) at the metal surface (R_f). From the values of polarization resistance (R_p) and double layer capacitance (C_{dl}) obtained from Nyquist plots and the calculated inhibition efficiency value (η %), it is obvious that the value of R_p increased with increasing concentration of inhibitor. The increase in R_p values is attributed to the formation of an insulating protective film at the metal/solution interface. It is also obvious that the value of C_{dl} decreased upon the addition of each of the inhibitors, indicating a decrease in the local dielectric constant and/or an increase in the thickness of the electric double layer suggesting that the inhibitors functioned by forming a protective layer at the metal surface. Generally, when a non-ideal frequency response is present, it is commonly accepted to employ the distributed circuit elements in the equivalent circuits. What most widely used is the constant phase element (CPE), which has a non-integer power dependence on the frequency [28, 29]. Thus, the equivalent circuit depicted in Fig. 8 is employed to analyze the impedance spectra, where Rs represents the solution resistance, Rt denotes the charge-transfer resistance, and a CPE instead of a pure capacitor represents the interfacial capacitance.

As seen from Table 3, the C_{dl} values decrease with the increase of LMS concentration, which suggests that LMS functions by adsorption on the mild steel surface. It is inferred that the LMS molecules gradually replace the water molecules by adsorption at the metal/solution interface, which leads to the formation of a protective film on the mild steel surface and thus decreases the extent of the dissolution reaction [30]. Moreover, the increase of LMS concentration leads to the increase of R_{ct} and η% values.

TABLE 4. Electrochemical parameters and inhibition efficiency (η%) obtained from polarization studies of mild steel in 2 M HCl solution in the presence and absence of LMS at 303 K.

Inhibitor	Concentration M X 10^{-4}	Ecorr Vm	Icorr μA cm^2	βc m V dec^{-1}	Ba μA m V dec^{-1}	η%
BLANK		510	1563	157	103	
LMS	0.1	-493	490	120	56	68.7
	5.0	-509	390	112	62	75.1

TABLE 5. Electrochemical impedance spectrocopy parameters and inhibition efficiency (η %) for mild steel in 2 M HCl solution in the presence and absence of LMS at 303 K.

Inhitor	Concentration M X 10^{-4}	Rp (Rct) Ω cm^2	f_{max}	C_{dl}	η%
BLANK		16.89	7.55	1248	
LMS	0.1	26.7	13.49	442	36.7
	5	38.7	17.77	231	55.9

3.5 Potentiodynamic polarization measurements

The anodic and cathodic potentiodynamic curves for mild steel in 2 M HCl solutions in the absence and presence of 1 x 10^{-5} M and 5 x 10^{-4} M of the **LMS** at 30^0C is shown in FIG. 2. The nature of the polarization curves remained the same in the absence and presence of the inhibitor, but the curves shifted towards lower current density in the presence of the inhibitor suggesting that the inhibitor molecules retard the corrosion process without changing the mechanism of thecorrosion process. The polarization curves exhibit cathodic and anodic polarization curves with well defined Tafel regions. The electrochemical parameters namely: corrosion potential (E_{corr}), corrosion current densities (i_{corr}), anodic Tafel slope (βa), cathodic Tafel slope (βb) and percentage inhibition efficiency (η %) determined from the polarization curves are summarized in Table 2 with a maximum value for 5 x 10^{-4}M concentration of the inhibitors at 303 K as 75.1%.

As observed, the corrosion potential (E_{corr}) has no definite shift and the corrosion current densities (i_{corr}) decreases when the concentrations of the inhibitors increase indicating that the inhibitors adsorped on the metal surface, and hence the inhibition efficiency increased with increasing inhibitor concentration causing small change in E_{corr} values implying that the inhibitors act as mixed type inhibitors affecting both the anodic and cathodic reactions. If the displacement in E_{corr} is more than ± 85 vM/SCE with respect to the corrosion potential of the blank, the inhibitor can be considered as cathodic or anodic type. If the change in E_{corr} is less than 85vM/SCE, the corrosion inhibitor can be regarded as mixed type [31, 32]. Maximum displacement is 31 vM/SCE which indicates that the inhibitor is mixed type.

3.6 Theoretical calculations

The optimized geometry of LMS is shown in Fig. 4 and their corresponding frontier molecular orbitals (HOMO and LUMO) are shown in Figs 5 and 6. The energy levels viz: E_{HOMO}, E_{LUMO} and ΔE calculated are depicted in Table 4. The energies of the frontier molecular orbital: E_{HOMO} and E_{LUMO} are significant parameters for the prediction of the reactivity of any chemical species. The frontier molecular theory describes that the formation of a transition state is due to an interaction between frontier molecular orbitals (HOMO and LUMO) of reacting species [33]. E_{HOMO} is associated with electron-donating ability of the inhibitor. As such, the inhibition efficiency of inhibitor is expected to increase with increasing value of E_{HOMO} since this indicates increasing ease of donating electrons to the vacant d-orbital of the metal. E_{LUMO}, on the other hand, is associated with the ability of the molecule to accept electron, therefore decreasing values of E_{LUMO} suggest better inhibition efficiency [34]. The energy gap of an inhibitor ($\Delta E = E_{LUMO} - E_{HOMO}$) is an important stability index and is used to develop theoretical models for explaining structure and conformation barriers in molecular systems. The smaller the energy gap, the better is the expected inhibition efficiency of the compound [35]. According to the results in Table 4, the highest value of E_{HOMO} -5.866 eV) and the lowest value of ΔE -0.906 eV) were found for **L- METHIONINE SULFONE (LMS)** affirming that **L-METHIONINE SULFONE (LMS)** has more potency to be adsorbed on the mild steel.The global hardness is the inverse of the global softness (η = 1/S). Values of S and η are presented in Table 4. The hard and soft acids and bases principle requires that a reaction between an acid and a base is favoured when global softness difference is minimal. Also, a hard molecule has a large energy gap while a soft molecule has a low energy gap.

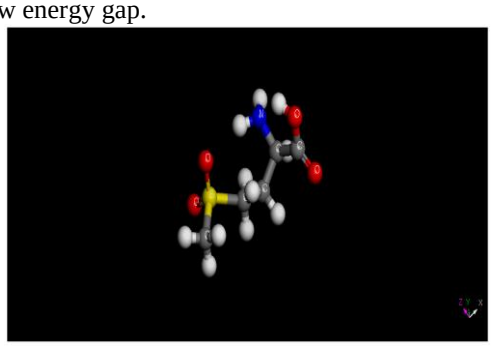

Fig. 7. DFT-B3LYP Optimized Structure of L - METHIONINE SULFONE.

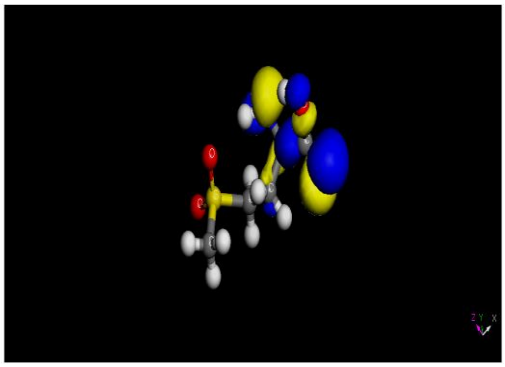

Fig. 8. HOMO electronic density of L - METHIONINE SULFONE molecule.

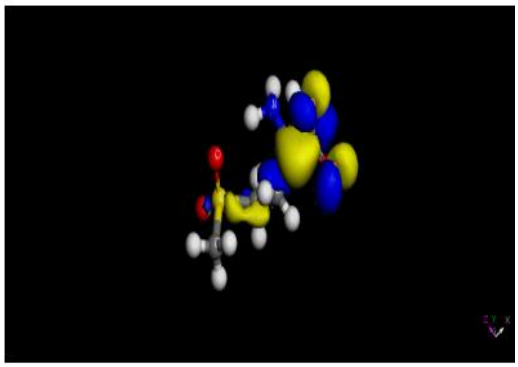

Fig. 9. LUMO electronic density of L - METHIONINE SULFONE (LMS) molecule .

Conclusion

1. **L - METHIONINE SULFONE (LMS)** showed good inhibition efficiency for the corrosion of mild steel in 2 M HCl solutions.
2. The corrosion inhibition is due to the adsorption of the inhibitor on the metal surface by physical and chemical adsorption.
3. The potentiodynamic polarization curves showed that the inhibitor is mixed type inhibitor.

TABLE 6. Quantum Chemical parameters for L - METHIONINE SULFONE (LMS).

Inhibitor	E_{HOMO} (eV)	E_{LUMO} (eV)	ΔE(eV)	Absolute electronegativity(eV)	Global hardness (eV)	Global softness (eV)
LMS	-5.866	-0.906	4.965	3.386	2.480	0.403

References

1. M. G. Fontana, N .D. Green, (1967) Corrosion Engineering. New York, McGraw - Hill Book Company
2. A. I. Onuchukwu, (2008) Electrochemical technology. Ibadan. Spectrum books limited.
3. I.B. Obot, N.O. Obi-Egbedi, Surf. Rev. Lett. 15(6) (2008) 903
4. X. Li, S. Deng, H. Fu, M. U. Guannan. Corros. Sci. 51 (2009) 620- 634.
5. L. Tang, X. Li, Y. Si, G. Mu, G.H. Liu, Mater. Chem. Phys. 95 (2006) 26.
6.A.Fiala, A. Chibani, A. Darchen, A. Boulkamh, K. Djebbar, Appl. Surf. Sci. 253 (2007) 9347.
7. S.S. Abd El-Rehim, H.H. Hassan, M.A. Amin, Mater, Chem. Phys. 70 (2001) 64.
8. A.S. Founda, A. Abd El-Aal, A.B. Kandil, Desalination 201 (2006) 216.
9. S.A. Umoren, I. B. Obot, I. E. Akpabio, S. E. Etuk. Pigment Resin Technol. 37 (2008) 98.
10.Y. Abboud, A. Abourriche, T. Saffaj, M. Berrada, M. Charrouf, A. Bennamara, N. Al Himidi,
Hannache. Mater. Chem. Phys. 105 (2007) 1.
11.I.B. Obot, N.O. Obi-Egbedi, Colloids Surf. A: Physicochem. Eng. Aspects 330 (2008) 207.
12. M. Lashkari, M. R. Arshadi, J. Chem. Phys. 299 (2004) 131.
13. I.B. Obot, N.O. Obi-Egbedi, Corros. Sci. 52 (2010) 198.14. N.O. Eddy, E.E. Ebenso, Int. J. Electrochem.Sci 5 (2010) 731.
15.P.C. Okafor, E.E. Ebenso, U.J. Ekpe, Int. J. Electrochem.Sci 5 (2010) 978.
16. K. F. Khaled, *Corrosion Science* 50: (2010) 2905 – 2916
17. I.B. Obot, N.O. Obi-Egbedi, Corros. Sci. 52 (2010) 198.
18. N.O. Eddy, E.E. Ebenso, Int. J. Electrochem.Sci 5 (2010) 731.
19.P.C. Okafor, E.E. Ebenso, U.J. Ekpe, Int. J. Electrochem.Sci 5 (2010) 978.
20. I.B.Obot, N.O. Obi-Egbedi, S. A. Umoren, E. E. Ebenso, Int. J. Electrochem.Sci 5 (2010) 994.
21. E.E. Ebenso, H. Alemu, S.A. Umoren, I.B.Obot, Int. J. Electrochem. Sci. 3 (2008) 1325.
22. N. O. Obi-Egbedi, I. B. Obot, Arab. J. Chem. (2010). doi:10.1016/Jarabjc.2010.10.004.
23. H. Ashassi-Sorkhabi, B. Shaabani, and D. Seifzadeh, *Applied surf. Sci.* 239 (2005)154 - 164
24. Umoren, S. A., Obot, I. B., Ebenso, E. E. and Okafor, P. C. *Portugaliae Electrochimica Acta* 26 (2008) 267 - 287
25. F. Mansfeld, M. W. Kendig, S. Tsai, Corros. Sci. 38 (1982) 570 – 580.
26. S. Martinez, M. Metikos-Hukovic, J. Appl. Electrochem. 33 (2003) 1137 – 1142.
27. F. Bentiss, M. Lebrini, H. Vezin, F. Chai, M. Traisnel, M. Laggrene, Corros. Sci. 51 (2009) 2165 – 2173.
28. J. L. Trinstancho-Reyes, M. Sanchez-Carrillo, R. Sandoval-Jabalera, V. M. Orozco-Carmona, F. Almeraya-Calderon, J. G. Chacon-Nava, J. G. Gonzalez-Rodriguez, A. Martinez-Villafarie, Int. J. Electrochem. Sci. 6 (2011) 419-431.
29. M. Kissi, M. Bouklah, B. Hammouti, M. Benkaddour, Appl. Surf. Sci. 252 (2006) 4190-4197.
30. F. Bentiss, M. Traisnel, M. Laggrene, Corros. Sci. 42 (2000) 127 – 146.
31. M. Yadav , D. Behera, S. Kumur, , R. R. Sinha, *Industrial and engineering chemistry research* 52 (2013) 6318 - 6328
32. M.. Yadav, S. Kumar, D. Behera,. *Journal of Metallurgy* 1 (2013) 1 - 15
33. K. Fukui, Springer-Verlag, New york, 1975.
34. G. Gokhan, Corros. Sci. 50 (2008), Pp. 2961 – 2992.
35. H. E. El Ashry, A. El Nemr, S. A. Esawy, and S. Ragab, Electrochim. Acta 51 (2006), Pp. 3957 – 3968.